Indian Journal of Pure & Applied Physics
Vol. 58, May 2020, pp. 409-414

Quasi-elastic scattering measurements of the ^{28}Si + ^{142}Nd system at back-angle

Saumyajit Biswas[a,b], A Chakraborty[a*], A Jhingan[c], D Arora[c], B R Behera[d], Rohan Biswas[c], Nabendu Kumar Deb[e], S S Ghugre[f], Pankaj K Giri[g], K S Golda[c], G Kaur[c], A Kumar[h], M Kumar[c], B Mukherjee[a], B K Nayak[i], A Parihari[c], N K Rai[h], S Rai[j], R Raut[f], Rudra N Sahu[k] & A K Sinha[l]

[a]Department of Physics, Siksha Bhavana, Visva-Bharati, Santiniketan 731 235, India

[b]Department of Physics, Murshidabad College of Engineering and Technology, Berhampore 742 102, India

[c]Inter University Accelerator Centre, Aruna Asaf Ali Marg, New Delhi 110 067, India

[d]Department of Physics, Panjab University, Chandigarh 160 014, India

[e]Department of Physics, Gauhati University, Guwahati 781 014, India

[f]UGC - DAE Consortium for Scientific Research, Sector III/LB-8, Bidhan Nagar, Kolkata700 098, India

[g]Department of Physics, Central University of Jharkhand, Ranchi 835 205, India

[h]Department of Physics, Banaras Hindu University, Varanasi 221 005, India

[i]Nuclear Physics Division, Bhabha Atomic Research Centre, Mumbai 400 085, India

[j]Department of Physics, Salesian College, Siliguri 734 001, India

[k]Department of Physics, IIT Ropar, Punjab - 140 001, India

[l]UGC - DAE Consortium for Scientific Research, Indore 452 017, India

Received 4 May 2020

The barrier distribution of a system can be extracted from excitation function data obtained either through fusion reaction or through quasi-elastic scattering measurement. In the present work, the quasi-elastic excitation function has precisely been measured at back angle for the ^{28}Si + ^{142}Nd system at energies around the Coulomb barrier and the corresponding experimental barrier distribution has been extracted. The experimental data has been interpreted in the frame work of the coupled channel calculations which include couplings to different possible modes of excitations of the interacting target-projectile combination. The possible effect of the nature of projectile excitations on the derived barrier distribution has been presented.

Keywords: Quasi-elastic scattering, Barrier distribution, Excitation function, Target deformation, Coupled channel calculation

1 Introduction

The study of the effect of couplings to the inelastic excitations of the interacting nuclei in the fusion process at energies around the Coulomb barrier has been carried out in several investigations over the last few decades. The investigations were made for a series of target-projectile combinations having different degrees of deformations[1]. The experiments were carried out involving the fusion and quasi-elastic excitation function measurements. Several interesting results governing the underlying fusion dynamics have come out from these investigations. It is to be noted that quasi-elastic scattering process of the heavy ion projectile like particles at the backward angles is considered to be the counterpart of the corresponding heavy-ion fusion reaction between the incoming projectile and the target. Both are inclusive processes and sensitive to the channel coupling effects at energies close to the Coulomb barrier. However, a major difference between the two processes is that the quasi-elastic scattering is related to the reflection probability at the Coulomb barrier, while the fusion is related to the transmission probability. The excitation function data reveals the most fundamental features of the underlying reaction process and is very often used for extracting the other relevant observable such as the extraction of barrier distribution. It is worthwhile mentioning that the barrier distribution of a given system obtained from both the quasi-elastic scattering and fusion excitation function measurements is found to be very similar in nature. However, the quasi-elastic excitation function measurement is relatively easier to carry out from the technical point of view

*Corresponding author (E-mail: anagha.chakraborty@visva-bharati.ac.in)

and there are also certain other advantages compared to that of fusion excitation function measurement[2]. Exploiting this fact, it has now become a common practice to use the excitation function data obtained from the quasi-elastic scattering events at large back angles for extracting the features of barrier distribution of the underlying reaction process.

In the present contribution, our main interest is to study the possible effects of coupling of different excitation modes of the deformed projectile, ^{28}Si, on the barrier distribution. It is expected that the dominance of a particular excitation mode of a deformed projectile in controlling a fusion process can be investigated in a comprehensive way with the use of a spherical target. The use of deformed target generally invokes the possibility for other coupling effects and may add up additional complexity. Hence, the present excitation function measurement and the follow up barrier distribution analysis have been carried out using the spherical ^{142}Nd target.

2 Experimental Details

The experiment was performed using the GPSC facility at IUAC, New Delhi. The accelerated beam of ^{28}Si was delivered by the 15 UD Pelletron accelerator. The beam energy was varied in the range of 84 (~ 30 % below barrier) to 136 MeV (~12 % above barrier). The enriched ^{142}Nd (98.26 % enrichment) target was used for the experiment. The effective areal thickness of the target was ~150 μg/cm^2. The target material was sandwiched properly between a carbon capping of thickness ~10 μg/cm^2 and a carbon backing of thickness ~25 μg/cm^2. The presence of capping and backing material helped in preventing the target from oxidization. The target was prepared at the IUAC target laboratory by evaporation process[3]. The scattered beam like particles were detected at the back angles using HYTAR[4] (HYbrid Telescope ARray) detectors. Each unit of the hybrid telescope detectors are comprised of ΔE and E detectors. The ΔE detectors are gas ionization chambers each of having an active length of 18 mm. The detectors were operated at 58 mbar pressure of isobutene gas during the experiment. The E detectors are passivated implanted planar silicon (PIPS) detectors each having a thickness of 300 μg/cm^2. Four telescope detectors, two in plane and the other two out of plane, each at an angle of 173^0 with respect to the incident beam direction were placed in a symmetrical cone like geometry. This arrangement was helpful in minimizing the uncertainty due to beam misalignment and obtaining data with good statistics within a relatively smaller amount of beam time. Two 300 μm thick silicon surface barrier detectors were kept at the angles of ±10^0 for beam monitoring and data normalization purposes. The excitation function measurements were carried out in 2 - 4 MeV energy steps in laboratory frame. The software packages, FREEDOM[5] and CANDLE[6] were used for the acquisition and the subsequent analysis of the acquired data. The counts for the quasi-elastic scattering events at a given beam energy and angle were extracted from the two-dimensional correlation plot of ΔE (energy loss) versus E (residual energy) obtained from the output signal of the corresponding hybrid telescope. A representative 2D plot of the spectrum obtained from the ΔE and E detector at θ_{lab}=173^0 for the incident beam energy of 116 MeV (in the lab frame) for the ^{28}Si + ^{142}Nd system is shown in Fig.1.

3 Data Analysis

As mentioned above, the present work is comprised of the measurement of the quasi-elastic scattering events for the ^{28}Si + ^{142}Nd system at back angle. It is to be noted here that the quasi-elastic events are defined as the sum of elastic, inelastic, and transfer events. The counts of interest have been extracted

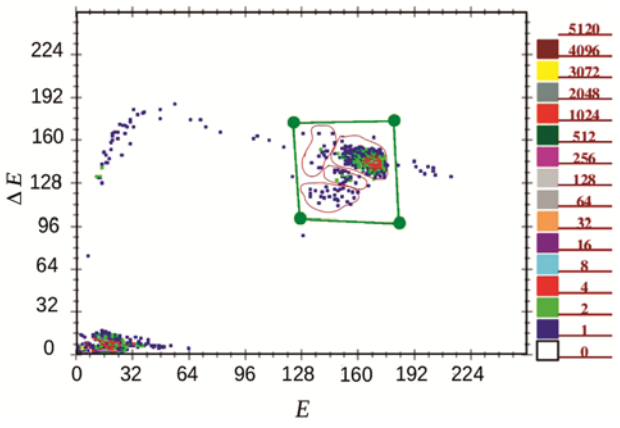

Fig. 1 — Representative two-dimensional correlation plot of ΔE-E energy signals (both are in channel numbers) from the hybrid telescope detector placed at 173^0 with respect to the beam direction. The figure corresponds to the data collected for the incident beam energy, E_{lab} = 116 MeV. The added counts from all the lobes have been considered to be due to quasi-elastic events. The regions of the different lobes are schematic only and have been drawn to guide the eye. The rectangular contour depicts the total region covering all the events of our interest (see text for details).

from the ΔE (energy loss) versus E (residual energy) plot (see Fig. 1). The ratio of the differential cross-section between quasi-elastic and Rutherford scattering events ($d\sigma_{qel}/d\sigma_R$) at a given beam energy and angle has been experimentally extracted using the standard procedure (see Ref. 7).The variation of this ratio as a function of incident beam energy (in cm frame) for the ^{28}Si+^{142}Nd system (quasi-elastic excitation function plot) is shown in Fig. 2. The figure depicts the quasi-elastic excitation function data measured at the angle of 173°. The uncertainties of the data points shown in the figure are statistical only. The typical values of statistical uncertainties associated with the data points lying at the lower and higher range of energies are found to be about 2 % and 5%, respectively. It is worthwhile mentioning that

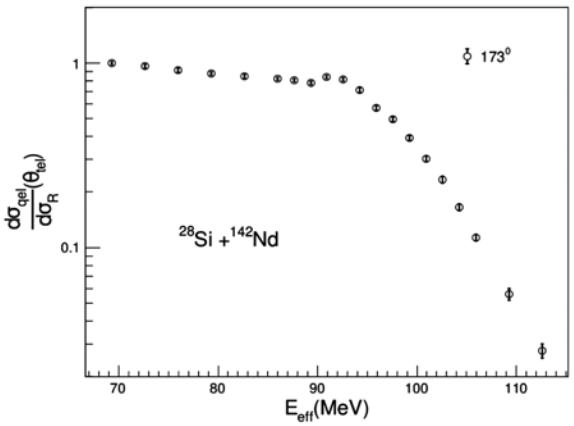

Fig. 2 — Quasi-elastic excitation function plot obtained from the present set of data recorded at 173^0 angle for the ^{28}Si + ^{142}Nd system.

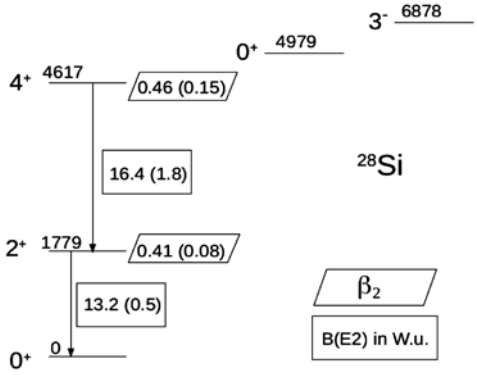

Fig. 3 — The low-lying level scheme of ^{28}Si highlighting the deformation (β_2) and the transition strengths (B(E2)) of the concerned states (see text for details). The position of level energy of 3$^-$ state is not according to the scale. All the spectroscopic data has been taken from the evaluated data base of ^{28}Si available in Ref. 13.

for the effective use of quasi-elastic excitation function data, measured at 173°, in extracting the corresponding fusion barrier distribution [D_{qel}(ε,173°)], one has to ideally carry out the measurements at 180°, which is physically not viable. In order to convert the results of $D_{qel}(\varepsilon, 173^\circ)$ to that of $D_{qel}(\varepsilon, 180^\circ)$, we have to introduce the effective energy (E_{eff}) term into the cross-section under the condition that $\sigma_{qel}(E_{eff}) \approx \sigma_{qel}(E_{c.m.}, 173°)$. The angle dependent centrifugal effects on cross-section get corrected through the use of E_{eff}. The corresponding value of E_{eff} can be obtained using the following relation[8]

$$E_{eff} = \frac{2E_{c.m.}}{1 + cosec(\theta_{c.m.}/2)}$$

where $E_{c.m.}$ and $\theta_{c.m.}$ denote respectively the beam energy at the half-target thickness position and the scattering angle in the centre of mass system. As mentioned in the aforesaid section, it has become now a well known fact that the fusion barrier distribution ($D_{qel}(\varepsilon)$) can be deduced experimentally from the corresponding quasi-elastic excitation function data $d\sigma_{qel}/d\sigma_R$. The relation, $D_{qel}(\varepsilon) = -d\,(d\sigma_{qel}/d\sigma_R)/dE$ (where $d\sigma_{qel}$ and $d\sigma_R$ are respectively the quasi-elastic and Rutherford scattering cross-sections at θ = 180°) and the standard point-difference formula[9] has been used to extract $D_{qel}(\varepsilon)$ from the measured excitation function data. The extracted barrier distribution plot obtained from

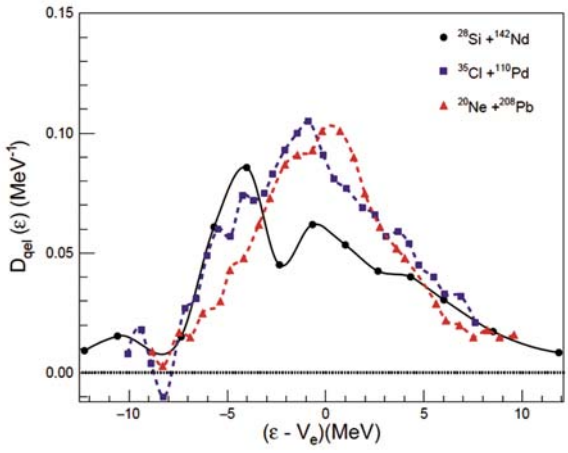

Fig. 4 — Comparison of the experimental barrier distribution for the systems ^{28}Si + ^{142}Nd (present work), ^{35}Cl + ^{110}Pd (from Ref. 7) and ^{20}Ne + ^{208}Pb (from Ref. 21). Due to the difference in the average experimental barrier (V_e) value for the three systems, the barrier distribution [D_{qel} (ε)] data has been plotted as a function of ε - V_e instead of ε.

the present measurement has been shown in Fig. 4 and 5. The experimental data shows two distinct hump like structure. It is notable here that the width of barrier distribution depends upon the coupling strength. The coupling strength for a system is found to be proportional to $Z_pZ_t\beta (= \omega)$, where Z_p and Z_t represents respectively the projectile and target nuclear charges and β denotes the average deformation parameter for the concerned system. Hence, different systems having similar ω value should exhibit the barrier distributions having almost the similar barrier width. This is evident from Fig. 4, where the width of the experimental barrier distribution for the present system has been compared with that of the other systems having the similar type of ω value. The relevant parameters for the three systems have been tabulated in Table 1. Although the fine structure pattern (which depends upon the additional microscopic features of the colliding nuclei) prevailing in the barrier distribution looks to be different for different systems, the three systems exhibit almost similar type of barrier width.

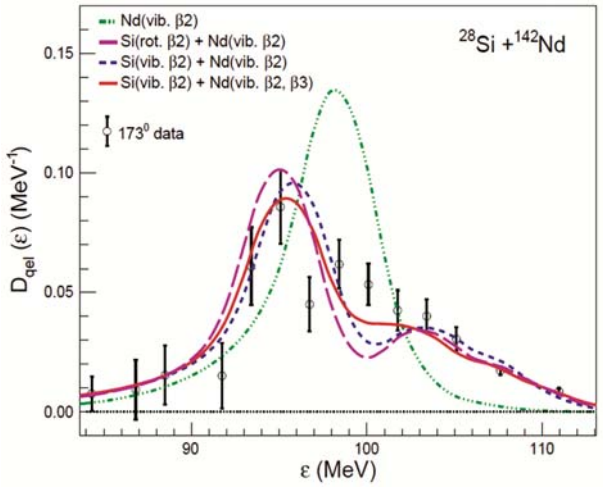

Fig. 5 — Comparison between the experimental and theoretical barrier distribution data for the ^{28}Si + ^{142}Nd system. The theoretical results have been obtained from the calculations using the CCFULL code under the different coupling schemes. The importance of the coupling of the vibrational effect of the projectile in reproducing the observed data is obvious from the figure.

4 Results and Discussion

For understanding the possible nuclear structure effects of the colliding nuclei on barrier distribution, theoretical calculations have been carried out using the quasi-elastic scattering version of the CCFULL code[10]. The Woods-Saxon type of nuclear potential, having a real and an imaginary part, has been used for the calculations. In the calculations, we have used an imaginary potential with the depth parameter of 30 MeV, the radius parameter of 1.0 fm, and the diffuseness parameter of 0.3 fm. The choice of the parameters is such that the imaginary potential lies well inside the Coulomb barrier with a negligible strength in the surface region. Under this condition, the calculated results were found to be insensitive to the parameters used for the imaginary part of the potential. For the real part of the nuclear potential, the potential depth V_0 is fixed at 190 MeV. The value of the radius parameter (r_0) is then adjusted for a particular value of the diffuseness parameter (a) in such a way that the Coulomb barrier height (V_b) becomes equal to that of the average experimental barrier (V_e). We have fixed the value of V_0 owing to the fact that the effect of variation in V_0 and r_0 on the Coulomb barrier height compensates for each other in the surface region. That is, for a given value of diffuseness parameter (a), the results do not significantly depend upon the actual choice of V_0, as long as the same barrier height (V_e) is maintained. The calculations have been performed using the value of r_0 as 1.1 fm and a_0 as 0.7 fm. The deformation parameters and the excitation energies of the projectile and target used for the calculations have been taken from Ref. 11 and12, respectively.

For the coupled-channel calculations, we have included the vibrational excitations for the spherical ^{142}Nd target nucleus in the harmonic oscillator limit. The choice of the excitation mode for the deformed ^{28}Si projectile is not straight forward and can be seen in the follow up discussion. The low-lying level structure of the incoming projectile, ^{28}Si has been depicted in Fig. 3. All the relevant spectroscopic parameters available in the literature have been

Table 1 — List of relevant parameters for the three systems.

System	Z_p	Z_t	β_2 (projectile)	β_2 (target)	Average β *	$Z_pZ_t\beta$
^{28}Si + ^{142}Nd	14	60	0.42	0.09	0.26	214
^{35}Cl + ^{110}Pd	17	46	0.23	0.26	0.25	192
^{20}Ne + ^{208}Pb	10	82	0.46	0.06	0.26	212

∗The value has been obtained from the average of values of β_2 (projectile) and β_2 (target).

presented in the figure. The experimental value of $E_x(4^+)/E_x(2^+)[E_x(2^+)$ and $E_x(4^+)$ represents the excitation energy of 2^+ and 4^+ state, respectively] is found to be 2.59. The theoretically expected value of $E_x(4^+)/E_x(2^+)$for a harmonic vibrator and rigid rotor is 2.0 and 3.33, respectively. Hence, the experimental level energy ratio of ^{28}Si lies in between the values expected for a pure vibrator and rotor[14] . On the other hand, the experimentally measured value of $B(E2: 4^+ \rightarrow 2^+)/B(E2: 2^+ \rightarrow 0^+)$ [*B(E2)* represents the *E2*-transition strengths between the corresponding two states] is 1.24 ± 0.14. This value is very close to the theoretically expected value (1.43) for an axially symmetric rotor; whereas the expected value for a perfect vibrator is 2.0. Hence, the low-lying level structure of ^{28}Si reveals the behaviour of neither a perfect rotor nor a perfect vibrator. In fact, the level structure of ^{28}Si has a long standing ambiguity related to the nature of its low-lying collective states[15 - 20]. Hence, the different possible excitation modes of the incoming projectile have been considered in the present calculations for the interpretation of the observed barrier distribution.

As a first step, the calculations with no coupling (considering both the target and projectile to be inert) have been carried out. This uncoupled calculation could not reproduce the experimental result. Next the vibrational coupling to the target (only the first 2^+ state) alone is included in the calculation. This calculation also fails to reproduce the experimental result (see Fig. 5). This indicates the importance for introducing the additional coupling modes to the projectile excitations. Indeed, we have obtained a better agreement between the experimental and theoretical results when the vibrational coupling to the first 2^+ state of the target and the coupling to the first 0^+, 2^+, 4^+ and 6^+ states of the ground state rotational band (under the rigid rotor limit) of the projectile is considered. It is to be noted here that the truncation of calculations at the 6^+ state is found to be sufficient enough as the calculated results do not seem to change much with the inclusion of states beyond the 6^+. The calculations have also been carried out with the vibrational couplings to the first 2^+ state of the projectile along with the vibrational excitation of the target to the first excited 2^+ state. The calculations indicate better results. However, the best fit to the experimental data is obtained only after the incorporation of vibrational excitation to the first 2^+ state of the projectile and the first 2^+ and 3^- states of the target nucleus in the calculation. It can thus be said that coupling effects to both the vibrational and octupole excitation modes of the target has a significant contribution in the observed barrier distribution. The calculated results also indicate the dominance of coupling of vibrational over the rotational degrees of motion for the incoming deformed projectile.

5 Conclusions

Barrier distribution for the ^{28}Si +^{142}Nd system has been deduced from the precisely measured quasi-elastic excitation function data at back-angle. The results from the coupled channel calculations show that the inelastic excitation of both the projectile and the target plays a significant role in the underlying fusion process. Further more, it has been observed that the experimental barrier distribution can be reproduced satisfactorily in the calculations with the consideration of ^{28}Si as pure vibrator in-spite of its large value of quadrupole deformation in the low-excitation regime. This supports the results of the previous works[19,20] carried out with ^{28}Si projectile and different target combinations. The present system has a positive Q-value of 1.244 MeV for the two neutron pick up channel (+2n). Hence, the influence of possible neutron transfer is also expected to have additional effect in the barrier distribution. This warrants further calculations with the possible couplings to neutron transfer channels as well.

Acknowledgement

The authors would like to thank the Pelletron staff of IUAC, New Delhi for providing the good quality beam during the experiment. Thanks are also due to D. Kabiraj and Abhilash S. R. for their help and support in preparing the targets. The authors are indebted to P. Sugathan for his help and all-round co-operation during the experiment. Thanks are also due to N. Madhavan and S. Nath for many helpful discussions and suggestions.

References

1 Dasgupta M, Hinde D J, Rowley N & Stefanini A M, *Ann Rev Nucl Part Sci*, 48 (1998) 401.
2 Hagino K & Rowley N, *Braz J Phys*, 35 (2005) 890.
3 Deb N K, Kalita K, Abhilash S R, Giri P K, Biswas R, Umapathy G R, Kabiraj D & Chopra S, *Vacuum*, 163 (2019) 148.
4 Jhingan A, Kaur G, Saneesh N, Ahuja R, Banerjee T, Dubey R, Singh V, Mahajan R, Thakur M, Kumar M, Yadav A, Behera B R & Sugathan P, *Nucl Instrum Methods Phys Res A*, 903 (2018) 326.

5 URL: http://iuac.res.in/ ~elab/das/ppdas/ Tutorials/fuman. html.
6 URL: http://www.iuac.res.in/NIAS/.
7 Capurro O A, Testoni J E, Abriola D, DiGregorio D E, Niello J O Ferna´ndez, Martı´ G V, Pacheco A J, Spinella M R & Ramı´rez M, *Phys Rev C*, 65 (2002) 064617.
8 Timmers H, Leigh J R, Dasgupta M, Hinde D J, Lemmon R C, Mein J C, Morton C R, Newton J O & Rowley N, *Nucl Phys A*, 584 (1995) 190.
9 Piasecki E, Kowalczyk M, Piasecki K, S´widerski Ł, Srebrny J, Witecki M, Carstoiu F, Czarnacki W, Rusek K, Iwanicki J, Jastrze¸bski J, Kisielin´ski M, Kordyasz A, Stolarz A, Tys J, Krogulski T & Rowley N, *Phys Rev C*, 65 (2002) 054611.
10 Hagino K, Rowley N & Kruppa AT, *Comput Phys Commun*, 123 (1999) 143.
11 Haouat G, Lagrange C, Swiniarski R, Dietrich F, Delaroche J P & Patin Y, *Phys Rev C*, 30 (1984) 1795.
12 Thornton S T, Schweizer T C, Gustafson D E, Ford J L C & Levine M J, *Nucl Phys A*, 270 (1976) 428.
13 URL: https://www.nndc.bnl.gov/.
14 Casten R F, Nuclear Structure from A Simple Perspective (Oxford University Press, New York), 1990.
15 Nayak B K, Choudhury R K, Saxena A, Sahu P K, Thomas R G, Biswas D C, John B V, Mirgule E T, Gupta Y K, Bhike M & Rajprakash H G, *Phys Rev C*, 75 (2007) 054615.
16 Kalkal S, Mandal S, Madhavan N, Prasad E, Verma S, Jhingan A, Sandal R, Nath S, Gehlot J, Behera B R, Saxena M, Goyal S, Siwal D, Garg R, Pramanik U D, Kumar S, Varughese T, Golda K S, Muralithar S, Sinha A K & Singh R, *Phys Rev C*, 81 (2010) 044610.
17 Danu L S, Nayak B K, Mirgule E T, Choudhury R K & Garg U, *Phys Rev C*, 89 (2014) 044607.
18 Khushboo, Mandal S, Nath S, Madhavan N, Gehlot J, Jhingan A, Kumar Neeraj, Banerjee Tathagata, Kaur Gurpreet, Devi K Rojeeta, Banerjee A, Neelam, Varughese T, Siwal Davinder, Garg R, Mukul Ish, Saxena M, Verma S, Kumar S, Behera B R & Verma P, *Phys Rev C*, 96 (2017) 014614.
19 Newton J O, Morton C R, Dasgupta M, Leigh J R, Mein J C, Hinde D J & Timmers H, *Phys Rev C*, 64 (2001) 064608.
20 Kaur G, Behera B R, Jhingan A, Nayak B K, Dubey R, Sharma P, Thakur M, Mahajan R, Saneesh N, Banerjee T, Khushboo, Kumar A, Mandal S, Saxena A, Sugathan P & Rowley N, *Phys Rev C*, 94 (2016) 034613.
21 Piasecki E, Swiderski Ł, Keeley N, Kisieli´nski M, Kowalczyk M, Khlebnikov S, Krogulski T, Piasecki K, Tiourin G, Sillanp¨a¨a M, Trzaska W H & Trzci´nska A, *Phys Rev C*, 85 (2012) 054608.